# Keratin modulation of autophagic flux in nutrient deprived HEK-293 cells

By: W. Zane Billings
Thesis advisor: Dr. Heather Coan

**Abstract**

Keratose is an oxidized form of keratin which can be extracted from hair, and is composed of alpha-keratin filaments and smaller gamma-keratins. Previous studies have shown keratin's ability to assist in burn healing and rescue stressed cells. Additionally, gamma-keratin was related to the upregulation of autophagy-associated genes in heat shocked cells, suggesting that the therapeutic value of keratin as a biomaterial may be explained by the induction of autophagy by keratins. Our study of keratin treatment in HEK-293 cells revealed that different protein treatments cause levels of fluorescent puncta (measuring the progress of autophagic flux in transfected cells) to change differently over time. Overall, our research suggests that keratin may be modulating autophagic flux, but slightly different experimental methods and further replication would make the link more clear.

Billings, W.Z. (2020). *Keratin modulation of autophagic flux in nutrient deprived HEK-293 cells* [Undergraduate thesis]. Western Carolina University.

Archived version from NC DOCKS available at: http://libres.uncg.edu/ir/wcu/listing.aspx?styp=ti&id=35521.

# Keratin modulation of autophagic flux in nutrient deprived HEK-293 cells

---

An undergraduate thesis
presented to the Faculty of the
Department of Biology

Western Carolina University
Cullowhee, North Carolina

---

In partial fulfillment
of the requirements for the degree
Bachelor of Science

---

W. Zane Billings

| | |
|---|---|
| Advisor: | Heather Coan |
| Committee: | Robert Youker |
| | Indrani Bose |

# Contents

# Abstract

Keratose is an oxidized form of keratin which can be extracted from hair, and is composed of alpha-keratin filaments and smaller gamma-keratins. Previous studies have shown keratin's ability to assist in burn healing and rescue stressed cells. Additionally, gamma-keratin was related to the upregulation of autophagy-associated genes in heat shocked cells, suggesting that the therapeutic value of keratin as a biomaterial may be explained by the induction of autophagy by keratins. Our study of keratin treatment in HEK-293 cells revealed that different protein treatments cause levels of fluorescent puncta (measuring the progress of autophagic flux in transfected cells) to change differently over time. Overall, our research suggests that keratin may be modulating autophagic flux, but slightly different experimental methods and further replication would make the link more clear.


# 1 Introduction

Keratins are a family of commonly occurring fibers which are constituents of human hair and nails, and compose horns, scales, and feathers in several animals. Keratins have been shown to assist in survival of human cells during stress events, and additionally, have been associated with the upregulation of several autophagy-associated genes. Autophagy is a mechanism by which unnecessary cell components are recycled into materials necessary for cell survival, and can be activated in the presence of stressors. Keratin shows potential as a biomaterial for the treatment of events associated with cell stress, and we hypothesize that keratin mediates the autophagy process, which accounts for keratin's ability to rescue stressed cells.

## 1.1 Keratin structure and function

Keratins are a class of intermediate filament-forming proteins which exhibit desirable qualities for bioengineering applications, and additionally do not provoke an immune response[1]. Keratins are the most abundant structural protein in epithelial cells[2], and form the major component of human hair and nails. Human keratins are composed of a long filamentous alpha-keratin which is associated with several smaller accessory proteins called gamma-keratins[3]. gamma-keratins are likely to display therapeutic potential and are the main candidate for the bioactive effects of keratin[4].

## 1.2 Keratin biomaterial extraction

Alpha and gamma-keratins tend to be more abundant in humans than beta-keratins. Specifically, alpha-keratin typically composes human hair and nails, while beta-keratins typically form scales, claws and beaks[3]. A crude mixture of keratins can be isolated from human hair via chemical extraction, and the crude mixture can be further refined to isolate only gamma-keratins. The crude keratin consists of keratin filaments, keratin-associated proteins, and enzymes, and can be extracted with a reducing agent from tissue[5].

Keratose, the oxidized form of keratins without disulfide cross-links, can be extracted from human hair by acid treatment, extraction, and dialysis. The resulting keratose can be stored

as a lyophilized powder which can be reconstituted by the addition of PBS (phosphate-buffered saline solution)[6].

## 1.3 Known effects of keratin on human cells

One of the main effects of keratin as a biomaterial therapy is due to the ability of keratins to self-assemble into scaffold structures. Keratins also possess the ability to bind to cells, creating a scaffold where cells can attach and proliferate[1]. Like other intermediate filament-forming proteins, keratins have a notable structural effect as part of the cytoskeleton[5], and additionally play a regulatory role. In particular, keratins, as part of the cytoskeleton, help to regulate cell size and proliferation, among other pathways[7].

Keratins have been observed to have a noticeable effect on mediating the survival of stressed cells *in vitro*, however no definitive mechanism for the ability of keratins to save stressed cells has been demonstrated. Keratin biomaterials have been shown to mediate recovery following burns[4,8], gamma-keratins display vasoactive properties[9], and keratin has also been linked to increased clearance of protein aggregates after stress events[10,11].

Furthermore, in a study of the effects of stem cell therapy for treating heart attacks, the use of keratin (extracted from human hair) as part of the therapy lead to keratin and stem cells rescuing heart cells following the heart attack, and additionally, the keratin scaffold alone, without stem cells present, was able to rescue stressed cells[12].

## 1.4 Keratin and autophagy

Additional studies have linked the presence of keratins in cell cultures with upregulation in transcription of autophagy-associated genes: gene expression panels of heat shock on cultured cells revealed that cell cultures treated with gamma keratose displayed upregulated genes associated with autophagy[4]. This result suggests that during times of stress, gamma-keratins may play a role in activating the autophagy pathway. If gamma-keratins can induce the upregulation of autophagy-associated genes, this may explain how keratins are able to rescue stressed cells.

## 1.5 The autophagy process

Autophagy, which literally translates to "self-eating," is a pathway wherein the cell collects unneeded material, including proteins and damaged organelles, into specialized recycling vesicles called autophagosomes (APs). There are three major types of autophagy: macroautophagy, where cytoplasmic contents are engulfed in specialized stored vesicles before being degraded; microautophagy, which involves cytoplasmic contents being brought directly into the lysosome; and chaperone-mediate autophagy, where chaperone proteins containing cargo are directed to lysosomes[13]. Hereafter, "autophagy" will be used to refer specifically to macroautophagy. The APs then fuse with lysosomes to form autophagolysosomes (APLs), wherein the waste contents are degraded (Figure 1). The small molecules leftover after degradation of waste products in the APL are then released into the cell where they can be used to produce new molecules which are more useful to the cell at the current time[14]. Autophagy can thus be thought of as recycling of cellular building materials.

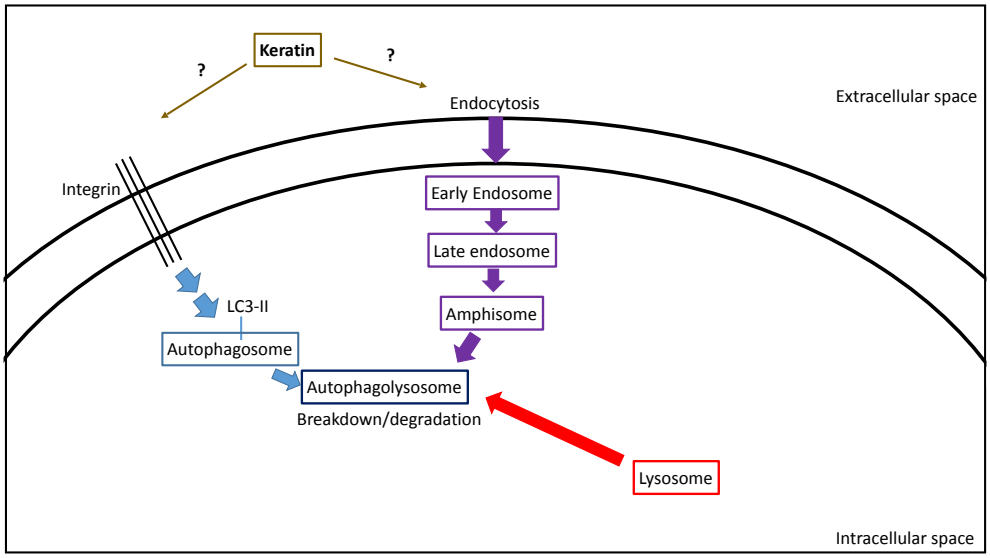


Figure 1: The autophagy process is a vesicle-mediated system for the degradation and recycling of components no longer needed by the cell.

During stress events, autophagy is upregulated in the cell in order to degrade unnecessary molecules, so the cell can devote more resources towards survival. For example, autophagy is upregulated during heat shock[15], so the cell can break down unneeded proteins in order to produce heat shock proteins and chaperones, which can assist in survival during a heat shock event. Autophagy is similarly upregulated during other types of stress, including nutrient starvation[16].

In order to monitor the effect of keratins on the process of autophagy in mammalian cells, a dual-reporter plasmid system was transfected into HEK-293 cells. The plasmid used[17] encodes the microtubule associated protein 1, light chain 3$\beta$ (LC3b) with two fluorophore tags at the N-terminus: EGFP, and mCherry. LC3b is commonly used as a biomarker of autophagic flux: under normal cellular conditions, the LC3b protein is free-floating in the cytosol (this cytosolic LC3b is referred to as LC3b-I), but upon the induction of autophagy, LC3b-I is conjugated with cytosolic phosphatidylethanolamine (PE; a type of phospholipid found in the cell membrane). The LC3b-PE conjugate, called LC3b-II, is then recruited to the membranes of autophagosomes[18].

Under control conditions where transfectant cells are growing normally, the tagged LC3b is constitutively expressed with no localization, so visualization of the cells using epifluorescence microscopy shows diffuse green and diffuse red fluorescence. When autophagy begins in the cells, APs form and LC3b is recruited to the membranes. As the tagged proteins aggregate into vesicles, small dots of intense fluorescence, called puncta, form in both the green and red channels. As the process of autophagy continues and lysosomes merge with APs to form APLs, the resulting acidic environment affects the chromophore of the eGFP tag,[17,19], and the green puncta disappear; if free-floating LC3b is still present in the cell, diffuse green fluorescence with green puncta will be visualized, but if all available tagged LC3b has been recruited to APs, only red puncta will be visualized. If all of the APs in the cell have fused and become APLs, only red puncta will be visible and there will be no notable green

fluorescence. If the cells remain under stress and stay in the autophagy pathway for too long, they will begin to die, and large amounts of red puncta will form as LC3b is collected in APLs for degradation (Figure 2).

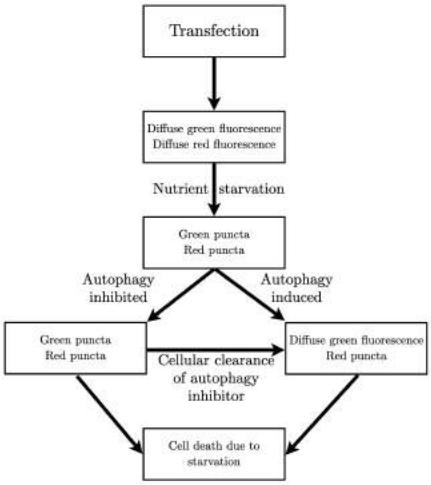


Figure 2: The dual reporter fluorescence system allows for the visualization of autophagy, due to its change in fluorescence patterns as autophagy progresses.

Keratins are a class of filamentous proteins which appear to have several useful properties for the creation of biomaterials; in particular, we hypothesize that keratins can activate the autophagy process in stressed cells. The induction of autophagy could help explain how keratin is able to ameliorate the negative effects of cell stress. As such, this study was intended to determine whether a relationship exists between the addition of keratin to stressed cells and the proportion of cells showing visible puncta at several time points. If stressed cells treated with keratin show a different trend over time in the proportion of cells with puncta, as opposed to untreated stressed cells, keratin may be modulating autophagic flux in stressed cells.

# 2 Methods and materials

## 2.1 Plasmid growth and extraction

Recombinant *Escherichia coli* cultures expressing the plasmid pBABE-puro mCherry-EGFP-LC3B were grown on LB-agarose (15 g/L agarose) plates with 100 ug/ml carbenicillin. The plasmid pBABE-puro mCherry-EGFP-LC3B was a gift from Jayanta Debnath (Addgene plasmid # 22418; http://n2t.net/addgene:22418; RRID: Addgene_22418)[17]. After 24 hours, individual cultures were picked from the plates and inoculated in LB liquid broth with 100 ug/ml carbenicillin. Liquid cultures were grown for a further 24 hours at 37 degrees Celsius while being shaken at 220 RPM. Plasmids were extracted from the liquid cultures using an Invitrogen™ Purelink™ Quick Plasmid Miniprep Kit (ThermoFisher). Purity and

concentration of plasmid isolates was examined using UV-Vis spectrophotometry; samples that appeared to be impure were discarded.

These methods were repeated for the plasmid EGFP-mApple (obtained as a gift from Dr. Robert Youker at Western Carolina University). For this plasmid, 100 ug/ul kanamycin was used instead of carbenicillin.

## 2.2 Growth and maintenance of HEK293 cell cultures

HEK293 cells, obtained as a gift from Dr. Robert Youker, were cultured in Gibco Dulbecco's Modified Eagle Medium (DMEM) supplemented with 10% Fetal Bovine Serum (FBS; Gemini Bio, Lot 900-108). Cells were passaged regularly at approximately 80% confluency, and were grown in a humidified incubator at 37 degrees and 5% CO2.

## 2.3 Plasmid transfection

HEK293 cells were transfected with plasmids using Continuum™ transfection reagent (Gemini Bio). Confluent HEK293 cells were seeded at $2 \times 10^5$ cells per well on a six-well cell culture dish.

Plasmid solutions were created using 100 µl of Opti-MEM™ reduced serum media (Thermofisher) and 500 ng of plasmid per well to be transfected. For most experiments, 1 well was transfected with mApple-EGFP and 5 wells were transfected with mCherry-EGFP-LC3B. A master mix of Continuum reagent was created by combining 100 µl of Opti-MEM with 2.5 ul of Continuum per well to be transfected. After allowing the solutions to incubate for 5 minutes at room temperature, 100 µl of the lipid master mix was added to each of the plasmid solutions per well to be transfected (e.g. if 5 wells were to be transfected with mCherry-EGFP-LC3B, 500 ul of lipid was added to that plasmid solution). The lipid-plasmid mixes were allowed to incubate at room temperature for 45 minutes. Then, 200 µl of the appropriate solution was added per well to the seeded 6-well dish. The dish was allowed to incubate for 24 hours in the humidified CO2 incubator.

Transfection was verified after 24 hours by visualizing the cells under the EVOS™ FL Auto epifluorescence microscope. If transfection was successful, the transfection media was aspirated off of the cells, cells were rinsed (gently) with PBS-D, and FluoroBrite DMEM phenol-free media (Gibco) was added to the cultures.

## 2.4 Protein treatment of cell cultures

After visualizing transfectants and taking pre-treatment images, different protein treatments were added to cell cultures.

The correct amount of the appropriate solution (Table 1) was added to the well after changing to the phenol-free media.

## 2.5 Nutrient starvation of cell cultures

For cultures which were starved, the protocol for transfection was followed until pre-treatment images were taken. After taking pre-treatment images, the phenol-free media was aspirated

| Substance | Concentration |
|---|---|
| Keratin (high) | 0.05 mg/ml |
| Keratin (low) | 0.01 mg/ml |
| Gelatin | 0.01 mg/ml |
| PBS-D | 0.005% (100 µl) |

Table 1: Concentrations used for protein treatments. PBS-D was added to be equal in volume to the gelatin addition.

off the cells and replaced with warmed PBS-D. Any necessary protein treatments were added at the concentrations described above and the cells were imaged again at designated time points.

## 2.6 Epifluorescence imaging of treated cultures

Images of treated and control cell cultures were taken at multiple time points (every 6 hours, up to 48 hours) using the EVOS™ FL Auto epifluorescence microscope. Both 16-bit monochromatic images, in both the green (GFP light cube) channel and red (TXRed light cube) channel (Table 2 shows the spectral compability), and an 8-bit pseudocolored overlay were taken with a scale bar (the EVOS system only allows native scale bars on 8-bit images). For every designated time point, 3 replicate image sets were taken of each well of the six well dish, each from different areas of the culture.

| | $\lambda_{ex}$ | $\lambda_{em}$ |
|---|---|---|
| GFP light cube | 477/22 nm | 510/42 nm |
| eGFP | 488 nm | 507 nm |
| TxRed light cube | 585/29 nm | 624/40 nm |
| mCherry | 587 nm | 615 nm |

Table 2: Emission/excitation maximum wavelengths for the light sources and fluorophores used. Both combinations are rated as "excellent" spectral matches by Thermofisher, the light source manufacturer[20]. Information about the fluorophores and light cubes was obtained from Dr. Robert Youker and from the light source manufacturer.

## 2.7 Data collection and analysis

Images were analyzed using FIJI (FIJI Is Just Image-J), a "Batteries-included" distribution of the Image-J analysis suite[21,22]. Only the EVOS-generated overlay images were analyzed, and the higher resolution monochrome images were saved as backups. The background noise was subtracted from the image using a 50-pixel radius rolling ball background subtraction algorithm, implemented in FIJI. The total number of cells in each image was counted, and the total number of cells with puncta in each image was counted. The count of cells with

puncta was divided by the total count of cells for each image to compute the proportion of cells with puncta in each image.

After data was collected, analysis was performed using R version 3.6.3[23] with `lme4`[24] and `lmerTest`[25]. Data cleaning and wrangling was performed with `readr`[26] and `dplyr`[27], along with `here`[28]. Plots were generated with `ggplot2`[29].

The data were examined for outliers in the response variable (proportion of cells with puncta) using Tukey's range method ($1.5 \times$ IQR) and none were found.

A linear mixed-effects model was used to analyze the results of the experiment. The proportion of puncta in each image was used as the response variable, explained by the fixed effects of time and treatment (and their interaction), and the random effect of the well. An ANOVA table was generated from the linear mixed effects model and used to interpret the model results. Satterthwaite's method was used to estimate the degrees of freedom, and the Nelder-Mead algorithm was used for optimization. Adding the well as a random effect accounts for the likely autocorrelation between measurements taken of the same well at different time points. Originally, repeated measures ANOVA was planned to analyze the data, but without further replicates, there are not enough degrees of freedom in the model to make conclusions about the treatment while considering the effect of repeated measures. All $p$-values were evaluated at the *a priori* significance level $\alpha = 0.05$.

# 3 Results

After several adjustments of the transfection method, a method was developed which typically results in bright, visible fluorescence in HEK-293 cells during all phases of autophagy. Several different parts of the method were adjusted, including the plasmid used, amount of transfection reagent, and amount of plasmid. Several repetitions of the experiment were performed, adjusting parts of the method each time–this included not only transfection optimization, but also time points for imaging and culturing methods. Only one replicate of the experiment was successfully completed using the finalized method. Representative cell images are shown in Figure 3.

Using the working transfection method, the various protein treatments were observed approximately every 6 hours for 48 hours. The mean proportions of puncta (Table 4) were analyzed in order to determine whether the protein treatments had a significant impact on the mean proportion of observed puncta. A profile plot of the group means is shown in Figure 4. On visual inspection, the proportion of puncta in each time:treatment combination appeared to be somewhat random. While the control, high keratin and low keratin treatments appeared to be mostly stable around 10–20% cells with puncta for the first 7 time points (pre-treatment to 36 hours), the PBS and gelatin treatments featured unpredictable spikes. In addition, the proportion of cells with puncta sharply increased in all treatment groups from 36 to 42 hours, and in all but one treatment group (high keratin) from 42 to 48 hours. Visually discerning between the treatments based on the profile plot was not possible, and the only time points with a noticeable visual pattern were 42 and 48 hours.

An ANOVA table was generated from the results of the linear mixed model (Table 3). The interaction between the time point and the effect of the treatment was significant.

Figure 3: Representative images of all cell cultures at each time point.

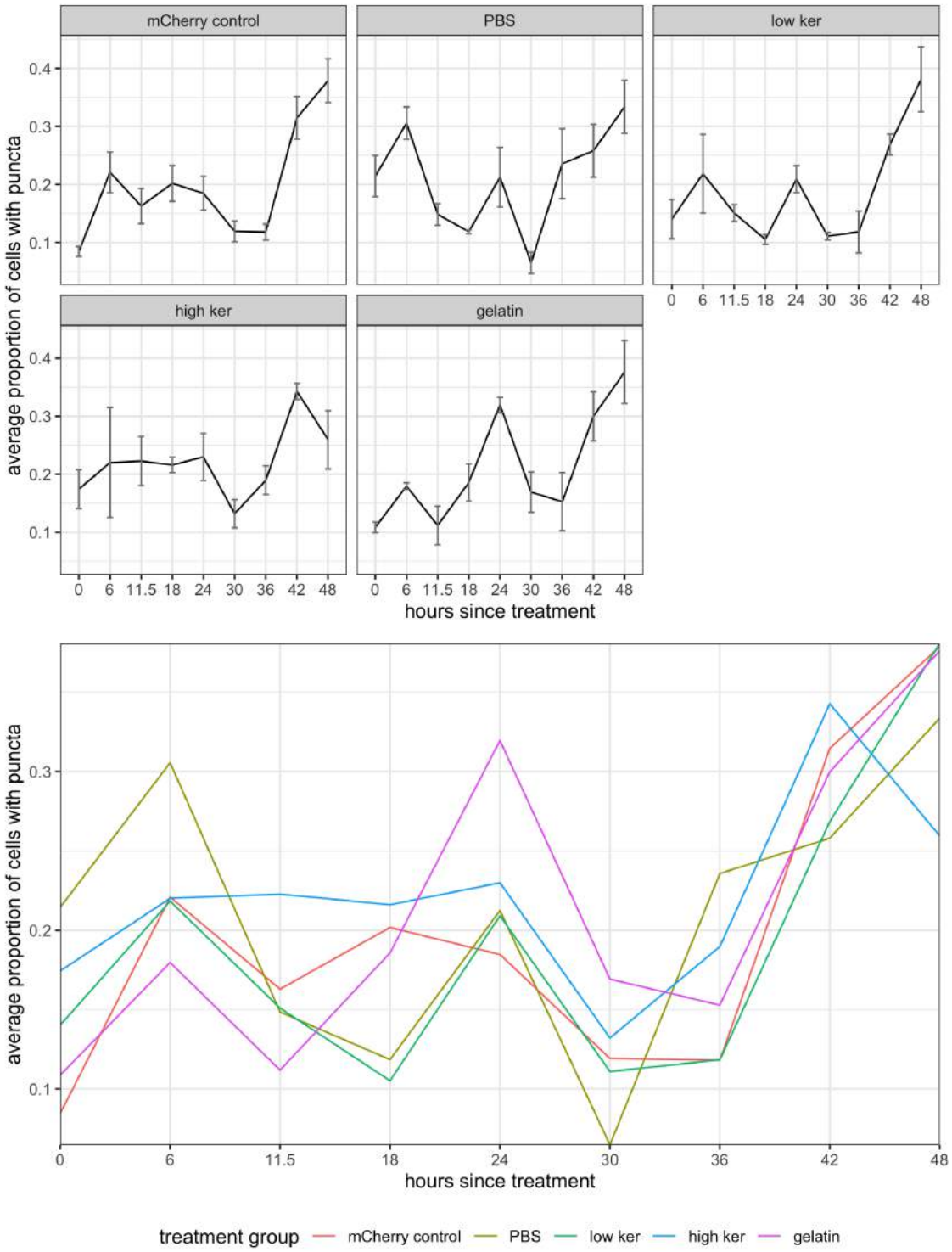


Figure 4: Profile plot of mean proportion of cells with puncta over time for each treatment. The curves are difficult to distinguish visually. The error bars show one standard error from the mean.

| Effect | Num. df | Den. df | $F$ | $p$ |
|---|---|---|---|---|
| treatment | 4 | 90 | 0.6247 | 0.6461 |
| time | 8 | 90 | 21.4514 | $< 0.0001$ |
| treatment:time | 32 | 90 | 1.6951 | 0.0274 |

Table 3: An ANOVA table was generated from the results of the linear mixed effects model. Note that the model produced a warning that it may not have fully converged.

# 4 Discussion

The interaction between treatment and time was significant, which indicates that each treatment likely behaves differently over the time points. In other words, just knowing the treatment or time point of an observation is not enough to make a conclusion about the response of that observation, but knowing the treatment and time point can be enough. Since the interaction is significant, interpreting the main effects (of treatment and time) is not reliable.

These conclusions align well with our hypothesis that keratin modulates the autophagy response of stress cells. Previous data from our lab have shown that cells treated with keratin can induce autophagy more rapidly than untreated cells

However, note that the model may not have converged (the specific error was "one eigenvalue is close to zero"). Due to the fact that each treatment was only represented by one well, there is not enough information to make a conclusion about the treatment. Since the estimation of the treatment effect is unreliable, the estimate of the interaction term may also be unreliable (although not necessarily; it is difficult to say definitively either way). Further replicates of the experiment should be conducted so that more than one well is present for each treatment. Then, accounting for the well as a random effect will address both autocorrelation of sequential measurements as well as possible uncontrollable variations in experimental conditions. With more than one well receiving each treatment, the linear mixed model analysis could be repeated with a better estimate of the treatment degrees of freedom, or repeated measures ANOVA could be used (while linear mixed models are more complicated, they are more flexible, and rANOVA is at most equivalent to a corresponding linear mixed model).

Additionally, we planned to include further controls in the experiment but were not able to due to time constraints. Positive controls to induce autophagy, such as chloroquine, 3MA, or rapamycin, among others, should be included in further replicates, although this will increase the number of measurements needed. Autophagy is also expected to increase in starved cells over time naturally, so choosing a smaller timeline with finer increments (e.g. every hour for 6 hours) may provide a better view of the process we are trying to study. In any case, more than one true replicate needs to be conducted as described previously.

Cell counting methods can also introduce a source of bias into the data. The number of cells in each picture were counted manually, as were the cells with puncta. Doing this manually relies on the analyst's discretion for what counts as a "cell" in the image, as well as for what constitutes puncta. Any bias by one particular analyst can be counteracted by having multiple people analyze the images independently, and then averaging (or otherwise

| | | Time | | | | | | | | |
|---|---|---|---|---|---|---|---|---|---|---|
| *Treatment* | *Repetition* | 0 | 6 | 11.5 | 18 | 24 | 30 | 36 | 42 | 48 |
| No Treatment | 1 | .0690 | .2857 | .1385 | .2632 | .2157 | .1538 | .1067 | .3864 | .4458 |
| No Treatment | 2 | .0984 | .2121 | .1268 | .1667 | .1264 | .0938 | .1023 | .2917 | .3158 |
| No Treatment | 3 | .0862 | .1648 | .2235 | .1756 | .2121 | .1102 | .1453 | .2660 | .3750 |
| | Mean | .0845 | .2209 | .1629 | .2018 | .1847 | .1193 | .1181 | .3147 | .3789 |
| PBS | 1 | .1489 | .3091 | .1702 | .1125 | .3063 | .0444 | .2833 | .3425 | .3924 |
| PBS | 2 | .2703 | .3519 | .1642 | .1221 | .1296 | .0938 | .3077 | .2458 | .3649 |
| PBS | 3 | .2241 | .2558 | .1111 | .1209 | .2014 | .1014 | .1163 | .1860 | .2439 |
| | Mean | .2144 | .3056 | .1485 | .1185 | .2124 | .0799 | .2358 | .2581 | .3337 |
| Gelatin | 1 | .0930 | .1698 | .1757 | .2404 | .3455 | .2178 | .0978 | .3433 | .3838 |
| Gelatin | 2 | .1250 | .1892 | .0638 | .1294 | .3108 | .1019 | .1081 | .2157 | .4659 |
| Gelatin | 3 | .1081 | .1800 | .0962 | .1875 | .3025 | .1180 | .2526 | .3407 | .2791 |
| | Mean | .1087 | .1797 | .1119 | .1858 | .3196 | .1459 | .1528 | .2999 | .3763 |
| Low keratin | 1 | .2075 | .2037 | .1786 | .1183 | .2136 | .1071 | .1237 | .2326 | .3333 |
| Low keratin | 2 | .1111 | .3421 | .1290 | .1087 | .1667 | .1026 | .1782 | .2857 | .3168 |
| Low keratin | 3 | .1020 | .1094 | .1452 | .0886 | .2472 | .1233 | .0531 | .2872 | .4925 |
| | Mean | .1402 | .2184 | .1509 | .1052 | .2092 | .1110 | .1183 | .2685 | .3809 |
| High keratin | 1 | .1389 | .2295 | .3014 | .2320 | .3034 | .0845 | .1593 | .3694 | .1831 |
| High keratin | 2 | .1429 | .0517 | .1571 | .2267 | .1630 | .1474 | .1714 | .3372 | .3544 |
| High keratin | 3 | .2414 | .3793 | .2099 | .1897 | .2234 | .1646 | .2385 | .3218 | .2410 |
| | Mean | .1744 | .2202 | .2190 | .2161 | .2299 | .1322 | .1897 | .3428 | .2595 |

Table 4: Proportion of cells with fluorescent puncta in each treatment group before treatment and every 6 hours for 48 hours after treatment.

combining) the results. Or, an automated method could be developed using FIJI in the future to eliminate this source of bias, although automated image analysis poses its own biases and issues.

In the future we also plan to not only count the number of cells with puncta, but to count two response variables, the number of cells with yellow puncta, and the number of cells with red puncta. Cells with yellow puncta indicate that LC3 has been recruited to autophagosomes, but autophagy has not progressed further, while cells with red puncta indicate that the autophagosomes have merged with lysosomes into APLs, causing the GFP tag to stop fluorescing. Monitoring both types of puncta separately may give a better picture of how the different protein treatments affect the progression of autophagy within the cell.

# 5 Acknowledgements

Dr. Robert Youker at Western Carolina University gifted us the eGFP-mApple plasmid as well as a HEK-293 starter culture. Dr. Mark van Dyke at Virginia Tech provided our lab with the keratin used. Dr. John Wagaman and Dr. Tom Martin at Western Carolina University provided advice on statistical analysis of the data. Dr. Indrani Bose (WCU) assisted with plasmid problems. Dr. Amanda Storm (WCU) provided several reagents. The Coan Lab group was instrumental in helping with experiments and cell culture maintenance.

# References

[1] Jillian G. Rouse and Mark E. Van Dyke. A review of keratin-based biomaterials for biomedical applications. *Materials*, 3(2):999–1014, February 2010.

[2] Pierre A Coulombe and M. Bishr Omary. 'Hard' and 'soft' principles defining the structure, function and regulation of keratin intermediate filaments. *Current Opinion in Cell Biology*, 14(1):110–122, February 2002.

[3] Sandleen Feroz, Nawshad Muhammad, Jithendra Ranayake, and George Dias. Keratin - based materials for biomedical applications. *Bioactive Materials*, 5(3):496–509, September 2020.

[4] Deepika R. Poranki and Mark E. Van Dyke. The effect of gamma keratose on cell viability in vitro after thermal stress and the regulation of cell death pathway-specific gene expression. *Biomaterials*, 35(16):4646–4655, May 2014.

[5] Hermann H Bragulla and Dominique G Homberger. Structure and functions of keratin proteins in simple, stratified, keratinized and cornified epithelia. *Journal of Anatomy*, 214(4):516–559, April 2009.

[6] Roche C. de Guzman, Michelle R. Merrill, Jillian R. Richter, Rawad I. Hamzi, Olga K. Greengauz-Roberts, and Mark E. Van Dyke. Mechanical and biological properties of keratose biomaterials. *Biomaterials*, 32(32):8205–8217, November 2011.

[7] Thomas M. Magin, Preethi Vijayaraj, and Rudolf E. Leube. Structural and regulatory functions of keratins. *Experimental Cell Research*, 313(10):2021–2032, June 2007.

[8] Deepika Rani Poranki. *Keratin biomaterial treatments for burn injury and mechanisms of tissue survival*. PhD thesis, Wake Forest University, 2012.

[9] Fiesky Nunez, Simon Trach, Luke Burnett, Rahul Handa, Mark Van Dyke, Michael Callahan, and Thomas Smith. Vasoactive Properties of Keratin-Derived Compounds. *Microcirculation (New York, N.Y. : 1994)*, 18(8):663–669, November 2011.

[10] Conner Davis. Keratin affects cellular pathways associated with autophagy in heat shocked human embryonic kidney cells, 2017.

[11] Robin Gardner. *Comparison of Protein Aggregate Formation by Different Stressors and in Various Cell Types*. Undergraduate, Western Carolina University, Cullowhee, NC, 2015.

[12] Deliang Shen, Xiaofang Wang, Li Zhang, Xiaoyan Zhao, Jingyi Li, Ke Cheng, and Jinying Zhang. The amelioration of cardiac dysfunction after myocardial infarction by the injection of keratin biomaterials derived from human hair. *Biomaterials*, 32(35):9290–9299, December 2011.

[13] D. Glick, S. Barth, and K. F. Macleod. Autophagy: cellular and molecular mechanisms. *J. Pathol.*, 221(1):3–12, May 2010.

[14] Eeva-Liisa Eskelinen. Maturation of Autophagic Vacuoles in Mammalian Cells. *Autophagy*, 1(1):1–10, April 2005.

[15] Karol Dokladny, Micah Nathaniel Zuhl, Michael Mandell, Dhruva Bhattacharya, Suzanne Schneider, Vojo Deretic, and Pope Lloyd Moseley. Regulatory Coordination between Two Major Intracellular Homeostatic Systems. *The Journal of Biological Chemistry*, 288(21):14959–14972, May 2013.

[16] Ryan C. Russell, Hai-Xin Yuan, and Kun-Liang Guan. Autophagy regulation by nutrient signaling. *Cell Research*, 24(1):42–57, January 2014.

[17] Elsa-Noah N'Diaye, Kimberly K Kajihara, Ivy Hsieh, Hiroshi Morisaki, Jayanta Debnath, and Eric J Brown. PLIC proteins or ubiquilins regulate autophagy-dependent cell survival during nutrient starvation. *EMBO Reports*, 10(2):173–179, February 2009.

[18] Isei Tanida, Takashi Ueno, and Eiki Kominami. LC3 and Autophagy. In Vojo Deretic, editor, *Autophagosome and Phagosome*, volume 445 of *Methods in Molecular Biology*. Humana Press, 2008.

[19] Tessa Campell and Francis Choy. The Effect of pH on Green Fluorescent Protein: a Brief Review. *Molecular Biology Today*, 2(1):1–4, 2001.

[20] Thermofisher. EVOS light cube selection guide, 2015.

[21] Johannes Schindelin, Ignacio Arganda-Carreras, Erwin Frise, Verena Kaynig, Mark Longair, Tobias Pietzsch, Stephan Preibisch, Curtis Rueden, Stephan Saalfeld, Benjamin Schmid, Jean-Yves Tinevez, Daniel James White, Volker Hartenstein, Kevin Eliceiri, Pavel Tomancak, and Albert Cardona. Fiji: an open-source platform for biological-image analysis. *Nature Methods*, 9(7):676–682, July 2012.

[22] Curtis T. Rueden, Johannes Schindelin, Mark C. Hiner, Barry E. DeZonia, Alison E. Walter, Ellen T. Arena, and Kevin W. Eliceiri. ImageJ2: ImageJ for the next generation of scientific image data. *BMC Bioinformatics*, 18(1):529, November 2017.

[23] R Core Team. *R: A Language and Environment for Statistical Computing*. R Foundation for Statistical Computing, Vienna, Austria, 2020.

[24] Douglas Bates, Martin Mächler, Ben Bolker, and Steve Walker. Fitting linear mixed-effects models using lme4. *Journal of Statistical Software*, 67(1):1–48, 2015.

[25] Alexandra Kuznetsova, Per B. Brockhoff, and Rune H. B. Christensen. lmerTest package: Tests in linear mixed effects models. *Journal of Statistical Software*, 82(13):1–26, 2017.

[26] Hadley Wickham, Jim Hester, and Romain Francois. *readr: Read Rectangular Text Data*, 2018. R package version 1.3.1.

[27] Hadley Wickham, Romain François, Lionel Henry, and Kirill Müller. *dplyr: A Grammar of Data Manipulation*, 2020. R package version 0.8.5.

[28] Kirill Müller. *here: A Simpler Way to Find Your Files*, 2017. R package version 0.1.

[29] Hadley Wickham. *ggplot2: Elegant Graphics for Data Analysis*. Springer-Verlag New York, 2016.